MFN= 007118
01 SID/SCD
02 5707
03 INPE-5707-PRE/1869
04 CEA
05 MC
06 am
10 Abdu, Mangalathayil Ali
12 Equatorial ionosphere-thermosphere system (EITS): an overview of recent results
14 349-361
18 Proceedings
40 En
41 En
42 <E>
53 STEP Symposium
54 <1992>
58 DAE
59 PROJETO IONO
61 <CI>
64 <1992>
68 PRE
76 AERONOMIA
83 The ionosphere - Thermosphere system of the earth's equatorial region Is governed by coupling processes peculiar to this region arising basically from the low inclination of the geomagnetic field coupled with the relatively larger fraction of the solar radient energy absorbed in the tropical latitudes. The major objective of the project EITS (of STEP/WG.3) is to study In detail the coupling processes of the system (a) under quiet conditions and (b) under EITS responses to solar wind - magnetosphere-high latitude ionosphere - thermosphere disturbances triggered by solar events, and to forcing from other atmospheric domains. the major phenomena of the EITS: the equatorial ionization anomaly -EIA (and the associated anomalies in wind, temperature and neutral densities), the equatorial spread F Irregularity processes - ESF, and the electrojet current system - EEJ, as well as the equatorial electric field and neutral winds are being Investigated using ground-based low latitude networks of radio, radar and optical Instruments by measurements conducted on board satellite and In rocket campaigns, and using theoretical/modelling studies on the coupling processes. The present overview will focus on recent results from EITS studies with specific focus on: coupling processes under quiet and disturbed conditions, equatorial electric fields based on measurements on plasma drift velocities and ESF,spread F plasma instability processes, neutral wind measurements, and longitudinal characteristics of disturbance penetration electric fields. Some outstanding problem to be focused using the data sets from the series of EITS campaigns being organized are also presented .
87 IONOSFERA
87 ELETROJATO EQUATORIAL
87 REGIAO EQUATORIAL
87 MAGNETOSFERA
90 b
91 FDB-19960313
92 FDB-MLR

RESUMO

A região de Alta Floresta, localizada na porção centro-oeste do Estado do Mato Grosso, apresenta como características um relevo plano, com intensa atividade antrópica e elevado potencial mineral (relacionado às mineralizações de ouro), mas possui poucos estudos geológicos e mapeamentos sistemáticos. Este trabalho tem como objetivo a avaliação de produtos de sensoriamento remoto integrados digitalmente (TM-Landsat/RADARSAT Standard, TM-Landsat/dados geofísicos gamaespectrométricos, RADARSAT/dados geofísicos gamaespectrométricos) para o mapeamento geológico e exploração mineral neste tipo de região. As imagens TM-Landsat e RADARSAT (S1 descendente e S3 ascendente) foram corrigidas geometricamente através do método de ortorretificação e integradas digitalmente através de realce por decorrelação e transformação *Intensity, Hue, Saturation* (IHS). A integração das imagens óptica e de radar com os dados geofísicos gamaespectrométricos (Contagem Total, Urânio, Tório, Potássio e as razões) foi baseada na aplicação da tabela de pseudo-cores e na transformação IHS. A avaliação do desempenho destes produtos integrados foi baseada na análise da contribuição de cada um deles para o mapeamento geológico. Os resultados deste trabalho mostram que estes produtos integrados possuem excelente desempenho na discriminação de vários domínios litoestruturais. As variações destes domínios nos produtos integrados TM e SAR/gama foram evidenciadas pelas cores e atributos texturais, que são bem relaciondas com as mudanças na geologia. Por outro lado, a integração das imagens RADARSAT com a imagem TM-Landsat foram importantes com relação ao maior realce de feições estruturais devido a geometria de visada do SAR (órbitas ascendente e descendente, com diferentes azimutes de iluminação) a ao azimute e elevação solar no imageamento do TM, de modo que esses produtos integrados foram complementares entre si. Sete domínios litoestruturais foram discriminados: embasamento, seqüência metavulcanossedimentar, rochas básicas, granitóides (granodioritos), rochas vulcânicas ácidas, granitos anorogênicos e uma cobertura metassedimentar (separada em três unidades), com idades variando do Arqueano ao Mesoproterozóico. Um importante *trend* de direção N60-70W e altos mergulhos relacionado às zonas de cisalhamento dúctil a dúctil-rúptil foi detectado e caracterizado através da interpretação visual dos produtos integrados e de dados de campo. Este trabalho mostra a importância de se utilizar imagens de sensoriamento remoto orbitais e dados aerogeofísicos integrados digitalmente para o mapeamento geológico, fornecendo também, o possível controle estrutural para as mineralizações auríferas da área.

From Proc. 1992 STEP Symposium

EQUATORIAL IONOSPHERE–THERMOSPHERE SYSTEM (EITS): AN OVERVIEW OF RECENT RESULTS

M. A. Abdu

National Institute for Space Research-INPE, P. O. Box 515, 12201-970 São José dos Campos, Brazil

ABSTRACT

The ionosphere - Thermosphere system of the earth's equatorial region is governed by coupling processes peculiar to this region arising basically from the low inclination of the geomagnetic field coupled with the relatively larger fraction of the solar radient energy absorbed in the tropical latitudes. The major objecive of the project EITS (of STEP/WG.3) is to study in detail the coupling processes of the system (a) under quiet conditions and (b) under EITS responses to solar wind - magnetosphere - high latitude ionosphere - thermosphere disturbances triggered by solar events, and to forcing from other atmospheric domains. The major phenomena of the EITS: the equatorial ionization anomaly -EIA (and the associated anomalies in wind, temperature and neutral densities), the equatorial spread F irregularity processes - ESF, and the electrojet current system - EEJ, as well as the equatorial electric field and neutral winds are being investigated using ground-based low latitude networks of radio, radar and optical instruments, by measurements conducted on board satellite and in rocket campaigns, and using theoretical/modelling studies on the coupling processes. The present overview will focus on recent results from EITS studies with specific focus on: coupling processes under quiet and disturbed conditions, equatorial electric fields based on measurements on plasma drift velocities and ESF,spread F plasma instability processes, neutral wind measurements, and longitudianal characteristics of disturbance penetration electric fields.Some outstanding problem to be focused using the data sets from the series of EITS campaigns being organized are also presentd.

INTRODUCTION

The earth's equatorial region has special significance in the solar-terrestrial energy program studies due to the relatively large fraction of the solar radiant energy input to the earth's sunlit hemisphere being absorbed in the tropical latitudes, and to the horizontal, or low inclination, orientation of the earth's magnetic field. Highest concentration in the quiet time global geoplasma distribution occurs in the tropical latitude in the phenomenon widely known as the equatorial ionization anomaly (EIA), or the Appleton anomaly. Other major phenomena arising from the dynamic coupling processes peculiar to this region are the equatorial electrojet current system (EEJ) and the equatorial spread F (ESF). A schematic of the functioning of the EITS, as far as these major phenomena are concerned, is presented in Figure 1. Under quiet conditions the solar tide induced zonal (and vertical) wind acting on the conducting magnetized ionospheric E layer plasma induces, through dynamo action, the electric field that drives the equatorial electrojet (EEJ), and the F region plasma drifts and the fountain effect that cause the anomalous distribution in the ionization, neutral densities, temperature and wind. The ionization anomaly produced by the EXB fountain effect has been the subject of rather extensive observational and theoretical modelling studies (e.g./1-6/). The latitudinal anomaly in the distribution of neutral densities were observed in the OGO-6 satellite measurements /7/. More recently, anomalies in the neutral air wind and temperature distributions closely related to the EIA were observed by Raghavarao et al /8/ from experiments (winds and temperature spectrometer and Langmuir probe) on board the DE-2 satellite. Meridional wind acts (Fig.1) mainly to control the latitudinal asymmetries of such anomalies. Although the anomalies in neutral densities, temperature

and wind represent evidences of the strong interactive coupling between the ionosphere and thermosphere, little is known about their possibly wide ranging characteristics, unlike in the case of the EIA.Although the EIA is a dominantly daytime phenomenon, it persists through a major part of the night depending upon season and solar activity /9/. The F layer dynamo electric field resulting from the sunset electrodynamic processes, and consequently, the well-known prereversal enhancement in the electric field /10,11,12,13,14/ is responsible for the evening/night time resurgence of the EIA /9/ as well as for the equatorial spread F (ESF) development /12,15/. During magnetospherically disturbed conditions globally coupled and large scale changes take place in the electric field /16/19/, thermospheric circulation, composition and temperature /17/ which in turn could cause drastic modification (including enhanced development or total inhibition) in the anomalies and ESF (/16,18,20/).

The major objective of the project EITS is to study in detail the coupling processes described in Fig. 1, taking into consideration the following two aspects: (a)- coupling within the system which is constantly operative and (b)- coupling to other regions which manifests itself through the EITS response to magnetosphere-high latitude ionosphere disturbances trigerred by solar events, and propagating atmospheric wave disturbances related, or not, to the former.We need to know more about the low latitude electric field and wind patterns and their controls on the behaviour of the major phenomena of the region under quiet conditions (of the aspect-a), and during geophysical disturbances (of the aspect -b). This is to be achieved by coordinated observations of the ionospheric and thermospheric parameters, including direct and indirect measurements of electric fields and neutral winds utilizing a variety of techniques and by theoretical/numerical modelling of the EITS coupling processes. The global distribution of the network of radio, radar and optical instruments utilized in the EITS project is shown in Table-1. Beside the routine operations of many of these instruments intensive observational schedules in campaign mode involve broader coverage of the existing instruments and in some cases in situ measurements onboard rockets.

TABLE 1 Ground-based Instruments Network Used in the EITS Campaigns

Ground-based instruments Network Used in the EITS Campaigns	AFRICAN SECTOR		INDIAN-ASIAN SECTOR				Others including Japan	PACIFIC SECTOR	AMERICAN SECTOR		
	W. Africa	Nigeria	India	China	Taiwan	Vietnam			Brazil	Peru	Argentina
Magnetometers	11[a]	9[a]	18[a]	2	1	4[a]	5	1	14[a]	11[a]	3
Ionosondes	4[a]	1[a]	4	1	1		5		2		1
Digisondes/Digital Ionosondes			3	1			1	1	1	1	
VHF Radars			1				1		1		
Incoherent Radars							1	1		1	
HF Radars	2		6		1		1				
Scintillations rxs.			18[a]								
TEC Polorimeters					3				3		
Optical Instruments (including scanning photometers and Fabri-Perot interferometers)	1		4						4		
Microputsation			3		1	1[a]					
Ionospheric Drift			3						1		
Geodetic Doppler					1						
Meteor Radar			1								
Partial Refl. Radar			1								

[a]Includes those operated during the IEEY period September 1991 March 1993
SATELLITES: GOES, DMSP, IMP8, UARS, NOAA/POLAR

The present overview concerns recent results from the EITS studies with specific focus on the following aspects: EITS coupling processes under quiet conditions; Equatorial electric field variations based on vertical and zonal plasma drift measurements and from ESF observations; Neutral wind measurements and determinations; EITS response to magnetospheric disturbances with implications on longitude asymmetry in the global disturbance electric field. Some preliminary results from the March-April 1991 EITS -1 coordinated campaign will be presented. This overview will conclude pointing out some of the outstanding problems of the EITS to be pursued.

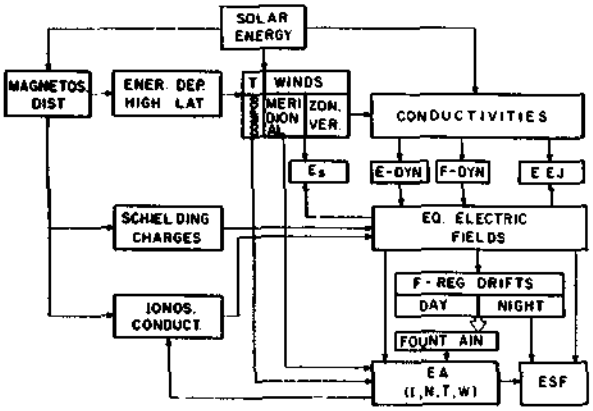

Fig. 1. A schematic on the EITS coupling processes.

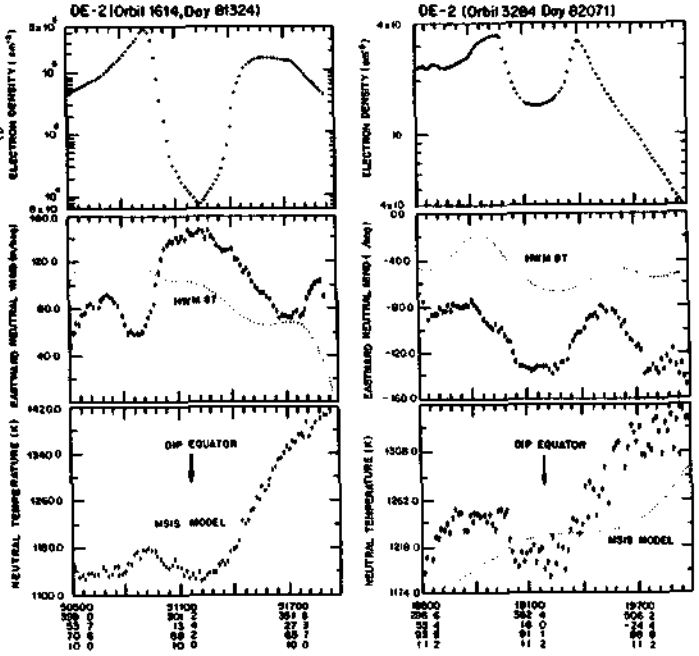

Fig. 2. Latitude profiles measured on DE-2 satellite of plasma density profile (upper panel) eastward neutral wind and neutral temperature (middle and botton panels) /8/, for 19LT (rightside) and 1112LT (left side).

EITS COUPLING PROCESSES UNDER QUIET CONDITIONS

Generation of electric fields by dynamo action driven by the neutral air wind, and the resulting electric currents, ion drifts, and the attendent ion and neutral drag forces constitute the basic interactive dynamic coupling processes that operate in the EITS. A clear manifestation of such a coupling process is evident in the equatorial temperature and wind anomaly observed from the DE-2 satellite data /8/. Fig. 2 shows the latitude distribution in the electron density, measured by a Langmuir probe (in the upper panel) and the neutral temperature and zonal wind (in the lower two panels) measured by the wind and temperature spectrometer on board the DE-2 (Dynamic Explorer) satellite during a high solar activity epoch. The well-known EIA represented by the trough at the magnetic equator straddled by two crests on either side is clearly seen in the top panels of the Fig.2 (for details on the hemispheric asymmetry present in all these parameters see /8/). The zonal wind (eastward in part-a for 1900 LT and westward in part-b for 1112 LT) shows maximum amplitude coincident with the EIA trough. The ion drag associated with the EIA produces the observed latitudinal distribution in the zonal wind (having negative correlation with electron density). This modulation in the zonal flow affects the energy balance and thus the latitudinal temperature variation as the bottom panels of the Fig. 1 a and b show. Here the increase (decrease) in the latitude profile of the temperature are collocated with the increase (decrease) in the ionization density.The higher (lower) damping at the crest (trough) results in

higher (lower) temperature and lower (higher) flow velocity for the neutrals resulting in the equatorial wind and temperautre anomaly (ETWA). The latitude anomalies in the neutral (N2 and O) densities mentioned above are related to the ETWA which present day models (e.g./21/) of the thermospheric wind and temperature do not predict. The latitudinal variation in the zonal wind could modify the F region dynamo electric field development with consequences on the ESF development processes /22,23/. Further, seasonal and solar cycle effects on the ETWA need to be understood in view of the well-known existence of such effects in the EIA.

EQUATORIAL ELECTRIC FIELDS:(A)-VERTICAL PLASMA DRIFTS

Extensive measurements of the vertical plasma drift (zonal electric field) over Jicamarca have brought out clearly the dependence of this drift on time of the day, season and solar and magnetic activities. Recent results /24/ of Fig. 3a show: (a)-little dependence of the daytime vertical drift on the solar (10.7 cm) flux values; (b)- relatively large degree of such dependences for nighttime drifts; (c)- large prereversal evening enhancements in the vertical drift for large solar flux values, the peak amplitude exceeding the day time values by a factor of ~2 in equinoctial and summer months of high solar flux(see also /25/; and (d)- seasonally the prereversal peak is always present except in winter months for solar flux values of less than ~100 units. The dependence of the evening prereversal drift velocity on solar flux is shown in Fig. 3b for different magnetic activity levels (represented by Kp values) /24/. Coley et al. /26/ observed from the AE-E satellite similar vertical ion drift velocities in longitude sectors of low and high B-values. This implied a corresponding longitude difference in the mean zonal electric fields. On the other hand, strong longitudinal asymmetry in the prereversal enhancement (zonal) electric field is present in the American longitude sector as the results of simultaneous measurement over Fortaleza (by ionosonde) and over Jicamarca (by radar) show in Fig. 4 (see also,/12,14,27/). An interesting aspect of the evening vertical electric field enhancement is the superimposed oscillations in its amplitude shown in Fig. 5a as observed from HF Doppler radar measurements over Trivandrum /28/. The power spectra of these oscillations in Fig. 5b shows dominant periods around 30 minutes which the authors /28/ attribute to modulation of the electric field by medium scale gravity waves. Such waves could undergo amplification leading to the triggering of spread F events /29,30,31/. However, in the few cases where such amplification was observed in /28/ no spread F was triggered, due possibly to the insufficiency of the ambient conditions such as the magnitude of the vertical drift velocity and the associated F layer height. Another important deciding factor for the triggering of the spread seems to be the requirement of a negative height gradient in the vertical drift. Such gradient in the vertical drift has been observed in the Jicamarca radar results /27/32/. Indirect evidence of the existence of such gradient, depending upon the season and magnetic declination angle of the observing station was obtained from a recent analysis by Abdu et al. /33/ of equatorial spread F distribution over Cachoeira Paulista for a eight -year period presented in Fig. 6a. The two minima in the plasma bubble/spread F occurrence rate (indicated by the dashed vertical lines) that occur near the middle of November and the end of January in the top panel of the figure are associated with the nodal points in the conjugate E layer sunset local times of the lower panel (Fig.6b). A physical explanation of the associated sunset electrodynamic processes depicted in Figs. 6c and d (see /33/ for details) could lead to the following situation: (a)- in Fig. 6c representing the simultaneous sunset at magnetically conjugate E layers, that is, perfect alignment of the sunset terminator with the magnetic meridian, an electric field uniform in latitude/height could lift up the F layer without substantially altering the bottomside electron density gradient as represented by the profiles 1, 2 and 3; (b)- for the situation in Fig. 6d that represent small deviation from a perfect alignment, that is, corresponding to the adjascent region away from the nodal points, the dynamo electric field that could decrease with latitude/height could cause the vertical uplift of the layer accompanied by systematic steepening of the bottomside density gradient; (c)- the situation (b) is more conducive to triggering of spread F than (a) thus explaining the occurrence of two minima in the spread F distribution. The role of a height gradient in the prereversal eastward electric field, such as that observed in the Jicamarca results /27,32/ is thus an additional requirement favouring the generation of the spread F irregularities. Further studies shoud be made to evaluate the relative role of such a gradient in the presence of the other ambient conditions mentioned above (including the amplitude of a perturbation source) for the R-T instability growth process. (See also, /34/).

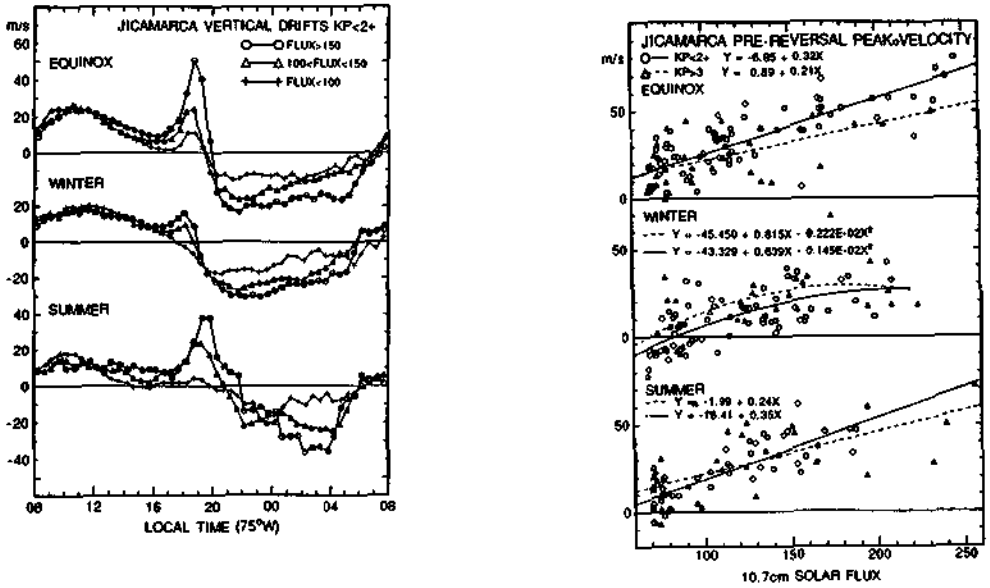

Fig. 3. (a)Average vertical plasma drift over Jicamarca.
(b)Preraversal velocity peaks as a function of solar flux for two levels of magnetic activity /24/

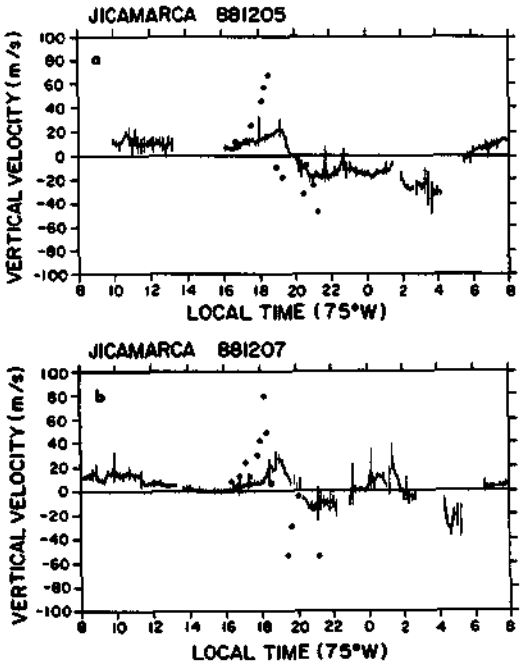

Fig. 4. Vertical plasma drift over Jicamarca for 5 and 7 December 1988. The solid dots are the vertical drift determined from Fortaleza ionograms for the same days.

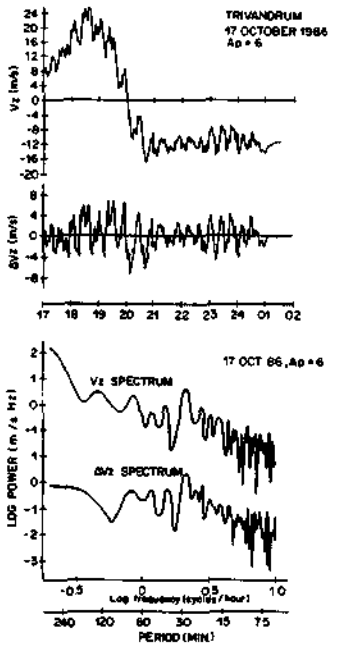

Fig. 5. Super imposed oscillations on the evening plasma vertical drift from HF Doppler radar over Trivandrum /28/.

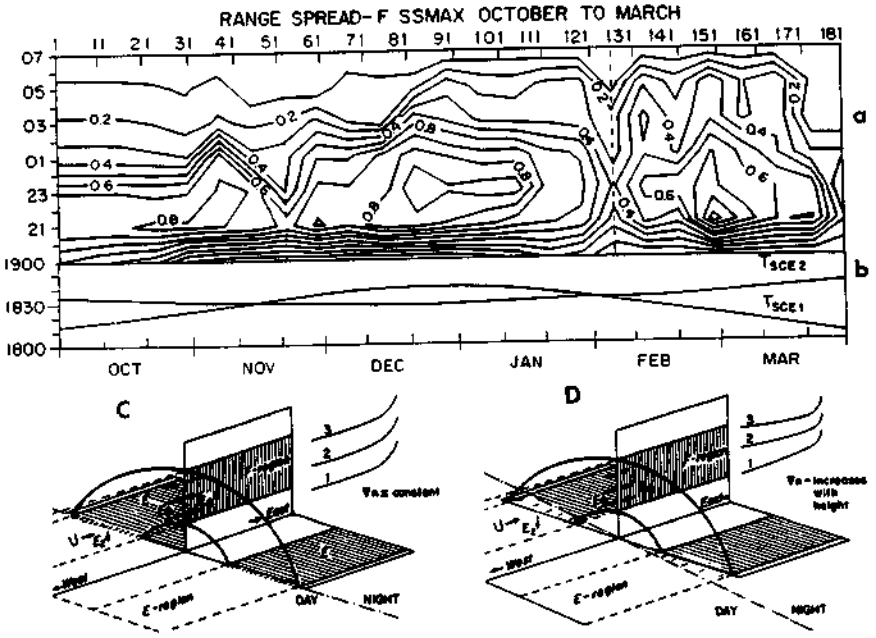

Fig. 6. (a)ESF distribution in local time versus day of the year plotted in percentage occurrences during 8 years, 1978-82 and 1988-90, representing solar maximum epochs. Vertical lines around the middle of November and early part of February indicate minima in the ESF occurrence associated with the nodal points in conjugate E-layer sunset times in (b). The sunset terminator and magnetic meridian geometry for their (c) perfect alignment and (d) daviation from perfect alignment. (see the text, also /33/).

(B)-ZONAL PLASMA DRIFT

Average zonal plasma drifts (that is, vertical electric field in the equatorial plane) published from Jicamarca measurements /24/ shows the following features: (a)-the westward drift from ~6 LT to ~17 LT is weakly dependent on the solar flux; (b)- the eastward drift that peaks arround 20-21 LT with amplitude significantly higher than the day time maximum shows significant positive dependence on solar flux; (c)-no such clear dependence on solar flux is present during the post midnight hours; (d)-the eastward drift shows negative dependence on the Kp index.

Fully developed and field aligned plasma bubble structures observed as depletions in 630 nm airglow profile over the low latitude location, Cachoeira Paulista, has been used /35/ as tracers of the the zonal plasma drift velocities. The results /35/ of eastward velocities measured in two photometer east-west scanning planes tilted +-30°off vertical are presented in Fig. 7. The velocities of the 30° N north plane is sistematically higher than that of 30°S. From equipotential field line considerations these results were interpreted by the authors as representing a negative height gradient in the zonal plasma flow in the equatorial plane. Comparison with the Jicamarca radar measurement /24/ for similar solar actvity epoch, also presented in Fig. 7 shows better agreement in the case of the 30°N velocities (that is, velocities around 540 km over the equator) than for the 30°S velocities (that corresponds to around 660 km over the equator). 630 nm Fabri Perot interferometer measurement of the zonal neutral wind /36/ over Cachoeira Paulista, are also plotted in Fig. 7. The velocities for the spring season compare well with the plasma drift velocities. More measurement of these velocities on a near simultaneous basis will be useful to establish quantitatively the differences that could arise among them depending upon the degree of decoupling between the E- and F- region and the resulting polarization electric field and field-aligned currents.

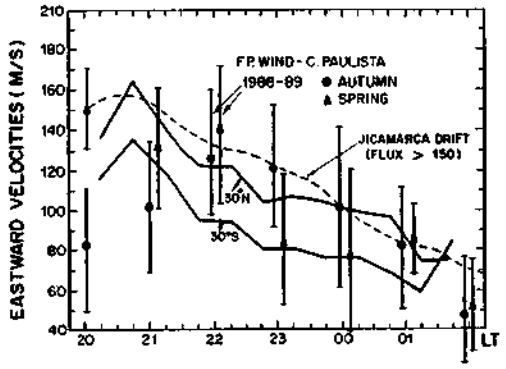

Fig. 7. Plasma bubble zonal velocities at 30°N and 30°S /34/ (solid line), F.P.I. zonal wind /35/ (dots with vertical bars), and Jicamarca average zonal drift velocity (dashed line) /24/.

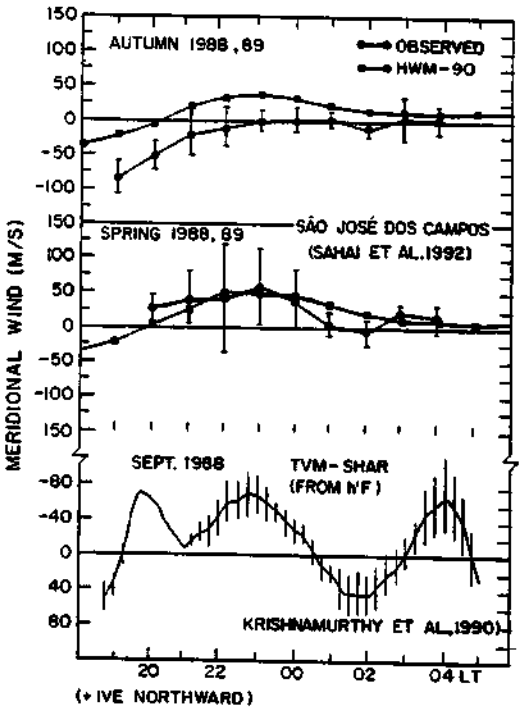

Fig. 8. F.P.I. meridional winds over Cachoeira Paulista /34/ for Autumn and Spring of 1988, 89 (top panels), and from spaced ionosondes over the equatorial region India /39/.

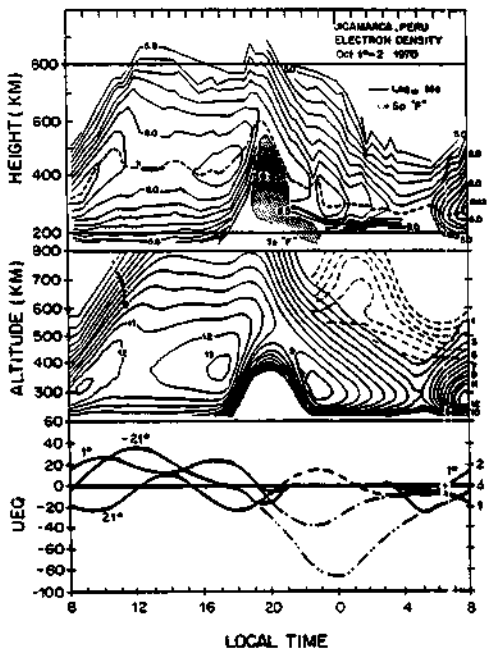

Fig. 9. Electron density distribution over Jicamarca measured by radar (top panel), and that simulated by Shefield computer code /43/ (middle panel), using the meridional neutral winds for 1°, 21° and -21° according to Hedin et al's modal /21/ (bottom panel). The dashed contours (in middle panel) resulted from Hedin et's winds around midnight shown in broken lines. Zero winds at these hours rsulted in better agreement between observed and modeled contours.

NEUTRAL AIR MERIDIONAL AND ZONAL WINDS

Besides the most widely used ground based direct measurement of thermospheric winds by Fabri Perot interferometer (F.P.I) technique /37/ there has been significant progress in terms of: (a)- satellite borne measurements (e.g./8,38/); (b)- indirect techniques based on comparison of ionosonde F layer peak height with its theoretical models /39,40/; and (c)- more sofisticated and complex computer codes such as the thermosphere general circulation models (TGCM's) and global scale ionospheric models. An example of the winds measured by DE-2 satellite /39/ showing anomalous latitude distribution was presented in Fig. 2. Comparison of ionogram hmF2 values with theoretical/model calculations of the peak height (for zero wind) has been used to determine meridional winds, with good measure of success over mid-latitudes /8/. Due to the dominating role of electric field this method has not been used over low latitudes. Comparison of the simultaneous h'F values measured by two ionosondes, one located at the dip equator (Trivandrum, 0.35'S dip) and the other at a station a few degrees away in latitude (at Sriharikota, 11°N dip) have been used by Krishnamurty et al. /40/to deduce the meridional wind. Their method makes use of the fact that the height variations of the F layer arising from the electric field effect are similar at the two stations where the effects from the meridional wind are dissimilar, and depend upon whether the wind blows northward or southward, the effect over the equator being negligible. The results of their calculation of wind presented as mean values representative of September 1988 plotted (with scale inverted) in Fig. 8 shows reasonably good agreement with F.P.I. results of meridional wind for identical epoch (spring 1988, 89 in the middle panel of this figure) /36/ for Cachoeira Paulista. An exceptional feature in the result from ionosonde is an enhancement in the southward direction centered around 20 LT. Simultaneous measurements by the F.P.I. and spaced ionosonde techniques will be useful to validate the latter tecnique.

A comparison was made /41/ between the meridional wind estimated from bottomside ionograms that made use of rocket borne measurement of ionosphere and thermosphere parameters, and that directly measured by the rocket vapour release experiment, and the agreement was good. In another study /42/ the F.P.I. wind over Mt. Abu (20°20'N) was used together with the servo model of the F2 layer to determine the peak height which was then compared with the hmF2 values measured by ionosonde over Ahmedabad (18°23'). The difference between the two sets of peak heights were attributed to the role of the electric field which was therefrom derived. More such comparison should be carried out and the characteristics of the resulting nocturnal electric field values need to be assessed further.

Thermospheric wind measurement by F.P.I. technique provides so far only night time winds. Development of dayglow measurement technique for low latitudes could be useful for covering the complete day. (Dayglow technique for monitoring of the EIA has been reported /43/). Besides the satellite-borne spectrometric technique, a promising one is certainly the use of detailed theoretical/numerical ionosphere-thermosphere models to explain the observed ionosonde and radar electron density distributions. As an initial step Bailey et al. /44/ used the detailed University of Sheffield computer code to model the electron density distribution measured by Jicamarca radar.They used the electric field simultaneously measured by the radar as one of the required input to the model and Hedin et al's /21/ thermospheric model wind as the other control input parameter. Their results presented in Fig. 9 show that the topside densities over Jicamarca around midnight hours is well reproduced if the low latitude meridional winds are zero at these hours which do not agree with the Hedin et al/21/ model winds for these hours(shown by broken lines), the inclusion of which would result in the topside density contours shown by broken lines in the middle panel of this figure. The Baily et al's /44/ modelled winds are in better agreement with the measurement by F.P.I. /36/ over Cachoeira Paulista.

EITS RESPONSE TO MAGNETOSPHERIC DISTURBANCES

It is now well established that different and more often complex types of electric field and wind effects are observed from disturbance solar wind-magnetosphere-high latitude ionosphere-thermosphere interaction processes depending upon the phase and intensity of the event (e.g. /16,45,46,47,48,49,50,51,52/). A recent review /18/ has focussed attention on disturbance effects on the ionization anomaly. The EIA can undergo drastic modification in the form of anomalous occurrences at local times outside that of its quiet time development and/or inhibition or enhancement at local times of its normal occurrences. Direct penetration to equatorial latitude of

magnetospheric electric field,and disturbance dynamo electric fields, winds and composition changes, produce significant alterations in the EIA spatial-temporal patterns as discussed in /18/. Case studies of the equatorial ionospheric response to disturbance electric fields based on simultaneous Jicamarca radar vertical drift observations and ionosonde h'F measurements /45,54/ have suggested the usefulness of the latter technique (in view of their wider global coverages), together with magnetograms, for diagnostics of the disturbance electric field effects on the EITS. Important aspects of transient electric field penetration to equatorial latitudes have been studied by Sastri et al. /51,52/ using F layer virtual heights from Indian ionosonde stations. Their results have identified important characteristics of the penetrating electric field over the equatorial latitudes arising from storm initial phase and substorm onset and recovery phases associated with southward and norhtward turnings respectively of the interplanetary magnetic field, Bz. The polarity structure of the disturbance electric field in these cases were in reasonable agreement with the global modelling results /45/ and with the radar results over Jicamarca /16/. Reddy et al. /54/ have used MU radar measurements and h'F values from the Japanese ionosonde station chain (representing low-mid-latitude conditions) to study substorm associated penetration electric field structure that was apparently at variance with the model predictions.

Important aspects of longitude dependence of the disturbance electric field have resulted from coordinated ionosonde and magnetometer measurements. Simultaneous EIA inhibition and EEJ current reversal in the Brazilian longitude sector in the morning was accompanied by EIA inhibition in the Indian afternoon sector and its enhanced development in the Asian evening longitude sector, the polarity of the day time westward electric field reversing to eastward in the evening sector /20/. An interesting case of the disturbance electric field longitude dependence during the 24-25 March 1991 storm event from the EITS-1 campaign is presented in Fig. 10. The storm onset in the Davao and Lumping magnetograms (bottom panel) is at 02 UT (10 LT). From 02 to 0530 UT (10 to 1330 LT) the enhanced H component over Davao suggests an enhanced eastward electric field (the nature of the large negative H deviation from 04 to 06 UT over Lumping is not clear). This eastward electric field is seen as hpF2 enhancements (till about 0630 UT) simultaneously over Hong Kong and Chung-Li(middle panel). The Fortaleza hpF2 and h'F values (in the top panel) in the night section show corresponding negative deviation from 23 to 02 LT. (Overall, the height variations manifesting the electric field effects are more pronounced during the night than during the day in both the Brazilian and Asian sectors). The height decrease starting at 0730 UT(0430 LT) over Fortaleza is caused by the sunrise effect. Complex height variations are present starting with the ring current enhancement onset near 21 UT at which there is large scale eastward electric field effects simultaneousy at all longitudes. In the Fortaleza sector this effect that followed a westward excursion of the electric field (downward height displacement,that was simultaneously present at other longitude as well) adds to the normal F layer dynamo field thus resulting in very large uplift of the layer (as compared to the quiet day behaviour shown dotted). This large uplift continued even after the E-field has reversed to westward over Asia. Thereafter the E-field oscillates in opposite phase at the two longitudes in the night (over Fortaleza) and day (over Asia) sectors.A clear demarcation of the longitude/local time of the disturbance E- field polarity reversal is difficult to determine from this example.

Marked longitudinal asymmetry in the equatorial ionosphere response to disturbance penetration E-field is evident in Fig. 11 that shows the h'F and hpF2 variations for 3 days around the great storm of March 1989 plotted for a number of equatorial low/ latitude stations in the order of their increasing westward longitude (the data used in this figure have been taken from /55,56,57/ (see also, /58,59/ for further results on EITS response to this storm). The vertical arrows in Fig. 11 represent the initiation of the quiet time evening prereversal electric field enhancements at each of the stations and solid dots indicate the midnights. Without going into many details of the figure the following major points may be commented:(a)- The nighttime eastward electric field enhancement is systematically more pronounced than the day time variations. This is not surprising due to the fact that photochemistry rather than electrodynamics dominates the day time variations. Also the lower heights(200-250 km) make the layer insensitive to westward electric field which requires downward movement of the layer to regions of increasing recombination rates. b)- The amplitude of the night time vertical displacement is significantly higher in the Brazilian sector (where the layer had disappeared for 2-3 hrs. from the 1000 km ionogram range) compared to those for the other longitudes. This longitude asymmetry has been observed also from the DMSP-9 passes in the region during this storm event by Greenspan et al./58/. Large precipitating proton fluxes in the region of the

south Atlantic anomaly accompanied these observations. More events should be analysed to study the details of such a longitude asymmetry in the EITS response features.

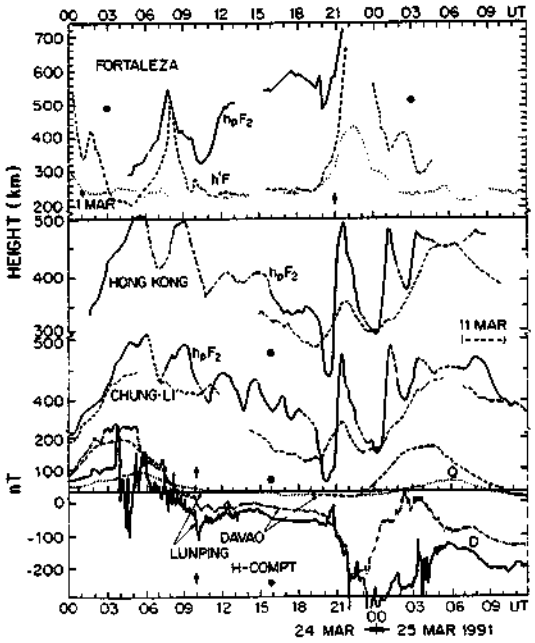

Fig. 10. F-region height parameters hpF2 and h'F over Fortaleza (top panel), hpF2 over Hong Kong and Chung-Li (middle panel) and H component magnetograms over Davao at Magnetic equator and Lumping at (35.2° dip). The datted and dashed lines represent quiet day variations.

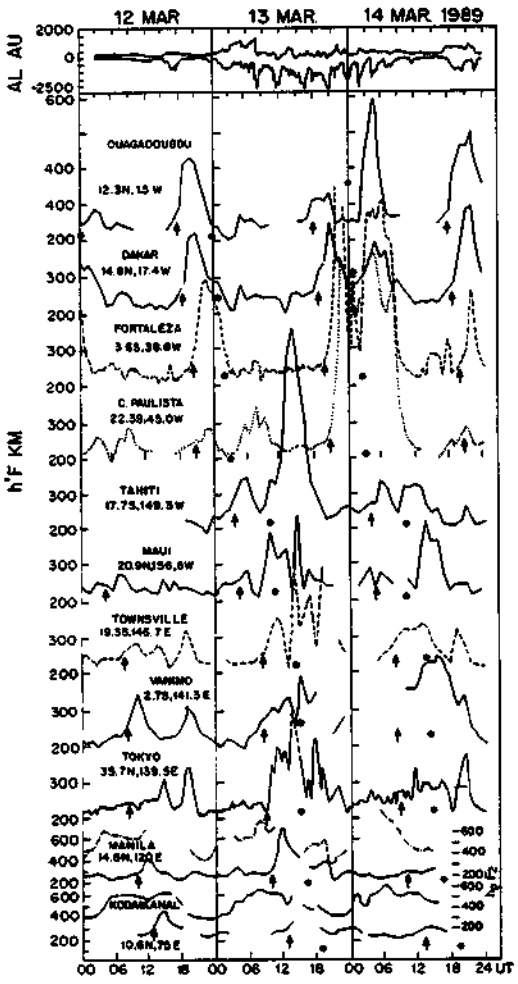

Fig. 11. Three-day plots (during the 13 March 1989 magnetic storm) of h'F values for equatorial-low latitude station for westward longitude increasing downward. For Manila and Kodaikanal hmF2 plots are also given. The top panel shows the Auroral activity indices AL and AU.

Equatorial anomaly could expand poleward to latitudes significantly away from that of the quiet time EIA crest during such disturbances.Total ionospheric electron content (TEC) data from low and middle latitudes analysed during the event of March 1989 show that anomalous increase by a factor ~2 in the TEC was observed in the American sector in geostationary satellite receiving paths from locations as far as ~40°N geomagnetic latitude, whereas the quiet time latitudianal limit of the EIA is confined to around +- 19°magnetic latitude (+- 38° dip) /60/. During this event the disturbance electric field over the equatorial latitude was > 6 mV/m, (as judged from Brazilain data /55/), that is, >6 times the quiet time value.

The disturbance E-field that cause anomalous uplift of the night F layer often triggers spread F/plasma bubble irregularity events. Although statistical studies have pointed to inhibition of the layer uplift and spread F in the evening-premidnight hours and a seasonally dependent enhancement in them in the post midnight hours/61/, case studies show that depending upon the phase of an

event rapid layer uplift accompanied by plasma bubble instability growth could occur both during evening as well as postmidnight hours /53,62,63/. Ring current associated electric field effect on the generation of scintillation irregularitues have been studied by Aarons /64/. From Jicamarca results Kelley and Maruyama /63/ have shown cases of instability growth rate condition existing for considerable durations (1-4 hrs.) starting from the onset of the layer drift reversal to upward all accompanied by spread F occurrences. Such conditions however do not seem to be valid for large scale events such as that of March 1989 during which neither the ground based scintillation receivers nor the DMSP ion density probe detected presence of significant irregularities. This problem merits further studies.

DISCUSSION AND CONCLUSIONS

Many important results on the EITS coupling processes have come out from recent investigations. They include (a) the ones mostly confined to within the EITS representing generally quiet conditions and (b) the coupling of the EITS to other regions that manifest itself in different forms of response of the system to solar, magnetospheric and high latitude ionospheric and thermospheric disturbances. Regarding the aspect (a) the most important task to be accomplished is certainly the development of a realistic electric field and neutral wind pattern valid for the different longitude sectors,season, and solar activity levels, notwithstanding the fact that the existing global models do provide valuable estimates of these parameters for equatorial latitudes as well. Different approaches presently being made by the scientific community in the way of providing input to such efforts include measurements of E-field and neutral winds by satellites and ground based techniques and detailed numerical modelling aiming at the use of these control parameters to explain observed features of the major the EITS phenomena. The studies on the disturbed EITS aim at understanding the detailed response of the system, especially that of its major phenomena, EIA, ESF and EEJ to different phases of a solar-interplanetary-magnetosphere disturbance event. A list of outstanding problems related to the EIA response to such disturbances has been given in the recent review by Abdu et al. /18/ and therefore they are not repeated here. Important aspects of the ESF irregularity processes that need to be understood concern the required amplitude for the initial perturbation sources that trigger them and the conditions under which the instability growth could be enhanced or inhibited. Such conditions include: 1- the role of zonal wind and conductivity structure that produce the evening prereversal E-field enhancement, the most basic precondition for the quiet time ESF generation; 2- height/latitude structure in the zonal electric field (vertical drift) and the associated development of the bottomside density gradient /33/; 3- possible role of meridional wind in controlling the instability growth /65/; 4- the required amplitude of an initial perturbation that will depend upon all the above factors especially on the aspect 2. Also, taking into consideration the high degree of sensitivity of the EEJ to magnetospheric and high latitude disturbances further studies should be carried out on the global character of the simultaneous responses of the EEJ and the EIA on the dayside and the ESF and the EIA on the nightside as function of the phase of a disturbance event. To conclude, the following is a list of problems to be focussed within the EITS campaigns that have already been conducted so far and those that are planned for the the immediate future: - Neutral wind and electric field pattern of the quiet and disturbed EITS; - EIA response as a function of substorm phases; - Longitude dependence in the disturbance magnetospheric electric fields; - Disturbance dynamo effects on EIA; - Ring current effects on EIA,EEJ andESF; - Possible global scale association among partial ring current developmentd EEJ reversal and EIA response; - Conditions for spread F instability growth and inhibition; Counter EEJ development conditions; - Geomagnetic and electric field pulsations in the EITS.

ACKNOWLEDGEMENTS

This work was partially supported by "Fundo Nacional de Desenvolvimento Cientifico e Tecnologico" of Brazil and by Conselho Nacional de Pesquisas Cientificas e Tecnologicas -CNPq through project no. 501956/91-3. I wish to thank all EITS project participants for providing me their preliminary results and preprints that were helpful in preparing this paper. Thanks are to Oulton Walker and Graham Baily for providing me their umpublished results.

REFERENCES

01. Moffett, R.J., Fun. cosmic Physics, 4, 313, 1979.

02. Appleton, E.V., Nature,157, 1946.

03. Rastogi, R.G., J. Geophys. Res., 64, 729, 1959.

04. Hanson, W.B., and R.J. Moffett, J. Geophys. Res., 71, 5559, 1966.

05. Walker,G.O., J.Atmos. Terr. Phys., 8,763,1981.

06. Abdu, M.A., G.O. Walker, B.M. Reddy, J.H.A. Sobral, B.G. Fejer, T. Kikuchi, N.B. Trivedi, and E.P. Szuszczewicz, Annales Geophysicae, 8, 419, 1990.

07. Hedin, A.E., and H.G. Mayr, J. Geophys. Res., 78, 1688, 1973.

08. Raghavarao, R., L.E. Wharton, N.W. Spencer, H.G. Mayr, and L.H. Brace, J. Geopys. Res. Lett., 8, 1193, 1991.

09. Anderson, D.N., J. Atmos. Terrest. Phys., 43, 753, 1981.

10. Rishbeth, H., Planet. Space Sci.,19 357, 1971.

11. Fejer, B.G., D.T. Farley, R.F. Woodman, and C. Calderon, J. Geophys. Res., 84, 5792, 1979.

12. Abdu, M.A., J.A. Bittencourt, and I.S.Batista, J.Geophys. Res., 86, 11443, 1981.

13. Farley, D.T., E. Bonelli, B.G. Fejer, and M.F. Larsen, J. Geophys. Res., 91, 13723, 1986.

14. Batista, I.S., M.A.Abdu, and J.A.Bittencourt, J. Geophys. Res., 91, 12055, 1986.

15. Woodman, R.F., J.Geophys. Res., 75, 6249, 1970.

16. Fejer, B.G., in:Solar wind-Magnetosphere Coupling, ed. Y. Kamide and J.A. Slavin, p.519, Terra Scientific, Tokyo, 1986.

17. Rishbeth, H., J. Atmos. Terr. Phys., 37, 1055, 1975.

18. Abdu, M.A., J.H.A. Sobral, E.R. de Paula, and I.S. Batista, J. Atmos. Terr. Phys. 53, 757, 1991.

19. Blanc, M., and A.D. Richmond, J.Geophys. Res., 85, 1669, 1980.

20. Abdu, M.A., G.O. Walker, B.M. Reddy, E.R.de Paula, J. H.A. Sobral, B.G. Fejer, E.P. Szuszczewicz, Annales Geophysicae, in press, 1992.

21. Hedin, A.E., M.A. Biondi, R.G. Burnside, G. Hernandez, R.M. Johnson, T.L. Killeen, C. Mazaudier, J.W. Meriwether, J.E. Salah, R.J. Sica, R.W. Smith, N.W. Spencer, V.B. Wickwar, and T.S. Virdi, J. Geophys. Res., 96, 7657, 1991.

22. Anderson, D.N., R.A. Heelis, and J.P. McClure, Annales Geophysicae, 5A(6), 435, 1987.

23. Aggson, T.L.N., N.C. Maynard, F.A.Herrero, H.G.Mayr, L.H. Brace, and M.C. Liebrecht, J.Geophys. Res., 92, 311, 1987.

24. Fejer, B.G., E.R. de Paula, S.A. Gonzalez, and R.F. Woodman, J. Geophys. Res., 96, 13901, 1991.

25. Balan, N., B. Jayachandran, R. Balachandran Nair, S.P. J. Atmos. Terr. Physics., 54, 1545, 1992.

26. Colev, W.R., J.P.McClure, and W.B. Hanson, J. Geophys. Res., 95, 21285, 1990.

27. Abdu, M.A., I.S. Batista, J.H.A. Sobral, B.G. Fejer, and E.P. Szuszczewicz, STEP Symposium/5th COSPAR Colloquium, John Hopkins University, 24-28, August 1992.

28. Balachandran Nair, R., N. Balan, G.J. Bailey, and P.B. Rao, Planet. Space Sci., 40, 5, 655, 1992.

29. Rottger, J., J. Atmos. Terr. Phys.,40, 1103, 1978.

30. Booker, H.G., J.Atmos. Terr. Physics, 41, 501, 1979.

31. Hysell, D.L., M.C. Kelley, and W.E. Swartz, J.Geophys. Res., 95, 17253, 1990.

32. Pingree, J.E., and B.G. Fejer, J. Geophys. Res., 92, 4763, 1987.

33. Abdu, M.A., I.S. Batista, and J.H.A. Sobral, J.Geophys. Res., 97, 14897, 1992.

34. Cole, K.D. J. Atmos. Terr. Phys., 36, 1099, 1974.

35. Sobral, J.H.A., and M.A. Abdu, J. Atmos. Terr. Phys. 53,729, 1991.

36. Sahai, Y., H. Takahashi, P.R. Fagundes, B.R. Clemesha, N.R. Teixeira, and J.A. Bittencourt, Planet. Space Sci., 40, 767,1992.

37. Biondi, M.A. J.W. Meriwether, Jr., B.G. Fejer, S.A. Gonzalez, and D.C. Hallenbeck, J. Geophys. Res., 96, 13901, 1991.

38. Herrero, F.A., H.G.Mayr, and N.W. Spencer, J.Atmos. Terr. Phys., 50, 1001, 1988.

39. Miller, K.L., D.G. Torr, and P.G. Richards, J.Geophys. Res., 91, 4531, 1986.

40. Krishnamurty, B.V., S.S. Hari, and V.V. Somayajulu, J.Geophys. Res., 95, 4307, 1990.

41. Sekar, R., and R. Sridharan, J. Atmos. Terr. Phys., in press, 1992.

42. Gurubaran, S., and R. Sridharan, J. Geophys. Res., Submitted, 1992.

43. Sridharan, R., S.A. Haider, S. Gurubaran, R.Sekar, and R. Narayanan, J. Geophys. Res., 97, 13715, 1992.

44. Bailey, G.J., R. Sellek, and Y Rippeth, Annales Geophysicae, submitted, 1992.

45. Fejer, B.G., M.C. Kelley, C. Senior, O. de la Beaujardiere, J.A. Holt, A. Teply, R. Burnside, M.A. Abdu, J.H.A. Sobral, R.F. Woodman, Y. Kamide, and R.Lepping, J.Geophys. Res., 95, 2367, 1990.

46. Reddy, C.A., V.V. Somayajulu, and C.V. Devesia, J Atmos. Terr. Phys., 41, 189, 1979.

47. Tanaka, T., Geophys. Res. Lett.,13, 1399, 1986.

48. Kikuchi, T., J. Geophys. Res., 91, 3101, 1986.

49. Somayajulu, V.V., C.A. Reddy, and K.S. Viswanathan, Geophys. Res. Lett., 14, 876, 1987.

50. Fesen, C.G., G. Crowly, and R.G. Roble, J. Geophys. Res., 94, 5405, 1989.

51. Sastri, J.H., K.B. Ramesh, and D. Karunakaran, Planet. Space Sci., 40, 95, 1992a.

52. Sastri, J.H., H.N.R. Rao, and K.B. Ramesh, Planet. Space Sci., 40, 519, 1992.

53. Abdu, M.A., B.M. Reddy, G.O. Walker, R. Hanbaba, J.H.A. Sobral, B.G. Fejer, F.F. Woodman, R.W. Schunk, and E.P. Szuszczewicz, Ann.Geophysicae, 6, 69, 1988.

54. Reddy, C.A., S. Fukao, T. Takami, M Yamamoto, T. Tsuda, Nakamura, and S. Kato, J. Geophys. Res., 95, 21077, 1991.

55. Batista, I.S., E.R. de Paula, M.A. Abdu, N.B. Trivedi, M.E. Greenspan, J. Geophys. Res., 96, 13943, 1991.

56. Lakshmi, D.K., B.C.N. Rao, A.R. Jain, M.K. Goel, and B.M. Reddy, Ann. Geophys., 9, 286, 1991.

57. Yeh, K.C., K.H. Lin, and R.O. Conkright, Can. J. Phys. in press 1992.

58. Greenspan, M.E., C.E. Rasmussen, W.J. Burke, M.A. Abdu, J. Geophys. Res., 96, 13931, 1991.

59. Huang, Y.N., and K. Cheng, J.Geophys. Res., 96, 13953, 1991.

60. Klobuchar, J.A., D.N. Anderson, and P.H. Doherty, Radio Science, 26, 1025, 1991.

61. Rastogi, R.G., J.P. Mullen, and E. MacKenzie, J. Geophys. Res., 86, 3661, 1981.

62. Szuszczewicz, E.P., B.G. Fejer, E. Roelof, R. Schunk, R. Wolf, R. Leitinger, M.A. Abdu, B.M. Reddy, J. Joselyn, P. Wilkinson, and R. Hanbaba, Annales Geophys. 6, 3, 1988.

63. Kelly, M.C., and T. Maruyama, A diagnostic model for equatorial spread F 2. J. Geophys. Res, 97, 1271-1277, 1992.

64. Aroons, J., Radio Science, 26, 1131-1149, 1991.

65. Maruyama, T., J. Geophys. Res., 93, 14611, 1988.